Available online at www.sciencedirect.com
SCIENCE DIRECT®
Journal of Photochemistry and Photobiology A: Chemistry 171 (2005) 113–120
Journal of Photochemistry and Photobiology A:Chemistry
www.elsevier.com/locate/jphotochem

Photocatalytic reduction of selenite and selenate using TiO_2 photocatalyst

Vi Nu Hoai Nguyen, Donia Beydoun, Rose Amal*

ARC Centre for Functional Nanomaterials, School of Chemical Engineering and Industrial Chemistry, University of New South Wales, Sydney, NSW 2052, Australia

Received 2 June 2004; received in revised form 25 August 2004; accepted 29 September 2004
Available online 11 November 2004

Abstract

The fate of selenite (Se(IV)) and selenate (Se(VI)) ions in illuminated TiO_2 suspensions was studied. In the presence of formic acid as a hole scavenger, both Se(IV) and Se(VI) were photoreduced to Se(0). The Se(0) deposited as either separate particles or a film on the TiO_2 particles. UV–vis reflectance measurements showed that the Se–TiO_2 powders were red-shifted relative to pure TiO_2 with an additional absorbance band at around 680 nm, attributed to Se(0). The photocatalytic reduction mechanism of selenium ions, with focus on selenite photoreduction, is discussed. It is proposed that direct reduction of Se(IV) by the electrons photogenerated in TiO_2 resulted in the formation of a Se(0) film while the formation of Se(0) particles was due to a chemical reaction between Se(IV) and Se(2−). The Se(2−) is believed to have been generated from the six electron photoreduction of Se(IV) and/or further photoreduction of Se(0) deposits.

Keywords: Selenite; Selenate; Photoreduction; Titanium dioxide; Mechanism

1. Introduction

Selenium is a naturally occurring trace element. Depending on its chemical form and concentration, selenium can be either essential or toxic to humans. In general, organic forms of selenium are more bioavailable, and less toxic than the inorganic forms (selenites and selenates) [1].

Selenium can exist in four different oxidation states: selenide (Se(2−)), elemental selenium (Se(0)), selenite (Se(IV)) and selenate (Se(VI)). Depending on the solution pH, these species can be present as Se(2−), SeO_3^{2-} and SeO_4^{2-}, and their protonated anions HSe^-, $HSeO_3^-$ and $HSeO_4^-$, respectively. As selenium has multiple oxidation states, it can participate in various redox reactions as shown in Table 1.

Due to anthropogenic activities, including mining, agricultural, petrochemical and industrial manufacturing operations, the level of selenium in the environment has increased [3]. Selenium that is present in wastewater can be removed using physical [4–7], chemical [8–11] and biological [12–14] treatment techniques. However, these techniques suffer some drawbacks. Physical removal techniques only concentrate the selenium compounds, with subsequent disposal remaining as a problem. Chemical processes often involve a high chemical cost. Biological treatment suffers from the inhibitory effect of the formed elemental selenium.

TiO_2-based photocatalysis has emerged as a promising technology for the degradation of various organic and inorganic contaminants. In principle, a photocatalytic reaction may proceed via the following steps: (a) generation of electron–hole pairs upon illumination of the TiO_2 with photons of energy greater than or equal to the band gap of the semiconductor; (b) trapping of the photogenerated electrons and holes within or on the surface of the TiO_2; (c) redox reactions induced by the electrons and holes with surface adsorbed species; (d) desorption of products and reconstruction of the TiO_2 surface. In a photocatalytic process, as the reduction and oxidation reactions occur simultaneously, organic compounds are often added as hole scavengers to allow for the reduction of the metal ions by the photogenerated electrons.

* Corresponding author. Tel.: +61 2 9385 4361; fax: +61 2 9385 5966.
E-mail address: r.amal@unsw.edu.au (R. Amal).

1010-6030/$ – see front matter © 2004 Elsevier B.V. All rights reserved.
doi:10.1016/j.jphotochem.2004.09.015

Table 1
Standard potentials of selenium redox couples (vs. NHE) (extracted from [2])

Chemical equilibrium	E^0 (V)	
Se(VI)/Se(IV) couple		
$SeO_4^{2-} + 3H^+ + 2e^- \Leftrightarrow HSeO_3^- + H_2O$	1.060	(1)
Se(IV)/Se(0) couple		
$HSeO_3^- + 5H^+ + 4e^- \Leftrightarrow Se^0 + 3H_2O$	0.780	(2)
$SeO_3^{2-} + 6H^+ + 4e^- \Leftrightarrow Se^0 + 3H_2O$	0.903	(3)
Se(0)/Se(2−) couple		
$Se^0 + H^+ + 2e^- \Leftrightarrow HSe^-$	−0.227	(4)
$Se^0 + 2e^- \Leftrightarrow Se(2-)$	−0.641	(5)

The photocatalytic reduction of selenite and selenate, with a greater emphasis on selenate, has been extensively studied using TiO_2 semiconductor as catalyst [15–21]. From such studies it has been found that in the presence of formic acid as a hole scavenger, selenium ions were photoreduced to their elemental form. In our previous study, we showed that using selenate as the precursor, spherical particles of Se(0) were formed on the TiO_2 particles and the formation of the Se particles due to the photoreduction of selenate ions was explained [18].

In this paper, the photocatalytic reduction of selenite is studied with an emphasis on investigating the formation and fate of Se(0) particles deposited onto TiO_2 during UV illumination. The photocatalytic reduction of selenate is also included for comparison. Formic acid is used as the organic additive in the present study since our earlier work demonstrated the effectiveness of this compound as a hole scavenger during Se(IV) and Se(VI) photoreduction [21].

2. Experimental

2.1. Chemicals

Sodium selenite, sodium selenate, sodium formate, formic acid, perchloric acid and sodium hydroxide were all of reagent grade and used as received. All water used was Milli-Q deionised water. TiO_2 Degussa P25 was used as the photocatalyst.

2.2. Apparatus

The photocatalytic experiments were performed in a glass reactor. This has been described in greater detail elsewhere [19]. Oxygen was evacuated from the system by purging with nitrogen. The contents of the reactor were magnetically stirred throughout the experiment. For each experiment, a 1 L reaction solution was illuminated by a 200 W Hg lamp, providing UV light of wavelength below 380 nm. In our previous study [21], it was found that the optimum pH for the photoreduction of selenite was 3.5. Therefore, the pH of the solution was maintained at 3.5. It should be noted that as the reduction of Se(IV) or Se(VI) could result in the production of toxic H_2Se gas, the reactor system was connected with two scrubbers in series, containing $CuSO_4$ and NaOH.

2.3. Procedure

A solution containing selenium ions (either as sodium selenite or sodium selenate), formic acid and the TiO_2 photocatalyst (at a loading of 1.5 g/L) were allowed to equilibrate for 20 min before irradiation. A 10 mL aliquot of this suspension was collected and immediately filtered through a 0.22 μm membrane filter. The filtrate was then analysed for selenium concentration (C_0). The dark adsorption was taken as the difference between C_0 and the initial concentration of selenium (C) added to the system. At the end of the 20 min dark adsorption period, the Hg lamp was switched on. The photoreaction period depended on the initial conditions in order to obtain similar concentrations of selenium ions remaining in the solution (C_i). Samples were taken at set time intervals and analysed for the concentration of selenium.

2.4. Analysis

A Perkin-Elmer Optima 3000 ICP-OES Spectrometer was used for selenium analysis. Each sample was analysed in triplicate. All analyses were obtained with relative standard deviation (R.S.D.) less than 3%.

2.5. Characterisation studies

High Resolution Transmission Electron Microscopy (HRTEM) images and elemental X-ray analysis were obtained using a Philips CM200 Electron Microscope. UV–vis reflectance measurements were carried out with Varian Carry 5 UV–vis–NIR spectrometer using $BaSO_4$ as a reference. The absorbance spectra were obtained from the reflectance measurements using the Kubelka–Munk relationship.

3. Results and discussion

3.1. Photoreduction of selenium ions

In a typical photoreduction experiment of Se(IV) and Se(VI) ions, the TiO_2 suspension colour changed from milky white to orange–pink, indicating the formation of elemental selenium. As the reaction proceeded, after 2 h of illumination (for an initial Se(IV) concentration of 20 ppm), 4 h of illumination (for an initial concentration of Se(IV) and Se(VI) of 40 and 20 ppm, respectively) and 8 h of illumination (for an initial Se(VI) concentration of 40 ppm), at which the selenite and selenate were almost exhausted from solution, black particles started to form in the $CuSO_4$ scrubber. This indicated the evolution of Se(2−) as H_2Se, which reacted with Cu^{2+} ions present in the scrubber to form the black CuSe particles. This has been reported in our previous studies [19–20]. Further illumination of the Se–TiO_2 suspension resulted in

Table 2
Selenite and selenate adsorption and photoreduction on TiO_2

Formic acid (ppm C)	100	200	300	400	600
Set 1: Se(IV) 20 ppm					
Adsorption (mg Se/gTiO_2)	6.4		6.9	6.3	6.2
Se remaining in solution after 2 h illumination (ppm)	1.5		1.1	1.9	1.6
Set 2: Se(IV) 40 ppm					
Adsorption (mg Se/gTiO_2)		7.7	8.3	6.8	5.2
Se remaining in solution after 4 h illumination (ppm)		3.7	2.2	2.7	3.2
Set 3: Se(IV) 80 ppm					
Adsorption (mg Se/gTiO_2)			9.7		
Se remaining in solution after 8 h illumination (ppm)			31.1		
Se remaining in solution after 13 h illumination (ppm)			1.24		
Set 4: Se(VI) 20 ppm					
Adsorption (mg Se/gTiO_2)	3.1	3.5	2.5		1.9
Se remaining in solution after 2 h illumination (ppm)	6.3	6.8	8.1		9.0
Se remaining in solution after 4 h illumination (ppm)	2.9	1.25	1.7		1.2
Set 5: Se(VI) 40 ppm					
Adsorption (mg Se/gTiO_2)	4.5	4.3	4.5		3.7
Se remaining in solution after 4 h illumination (ppm)	16.3	15.4	17.2		15.6
Se remaining in solution after 8 h illumination (ppm)	2.7	1.6	1.5		1.2
Set 6: Se(VI) 80 ppm					
Adsorption (mg Se/gTiO_2)			4.2		
Se remaining in solution after 8 h illumination (ppm)			46.6		
Se remaining in solution after 18 h illumination (ppm)			1.6		
R.S.D. (%)			3		

more black particles being formed in the scrubber while the orange–pink colour of the suspension gradually faded.

Results on the adsorption and photocatalytic reduction of selenite and selenate in the presence of various concentrations of formic acid as a hole scavenger are presented in Table 2. Note that the formic acid concentrations are reported as total organic carbon (ppm C). The largest dark adsorption and photoreduction of selenite for both 20 and 40 ppm initial concentrations occurred when 300 ppm C formic acid was added to the system (Sets 1 and 2). Our previous study [19] found that there was an optimum formic acid concentration for the photoreduction of selenate. This was attributed to competitive adsorption between selenate and formate ions on the positively charged TiO_2 particles, and subsequent photoreduction of selenate to elemental selenium. This could also be the case for selenite photocatalytic experiments.

Compared to selenite, in the presence of the same formic acid concentration, selenate (Sets 4 and 5, Table 2) demonstrated poorer adsorption on TiO_2. Furthermore, for the same initial concentration, selenate removal required double the time taken to remove selenite to a similar amount. The difference in the removal of selenite and selenate can also be seen in Fig. 1.

As can be seen from Fig. 1, for an initial concentration of 20 ppm, a large removal of selenite was achieved in the first 60 min (line a, Fig. 1). On the other hand, the removal of 20 ppm selenate proceeded more slowly (line c, Fig. 1). At this initial concentration, complete ion removal was achieved after 120 min for the selenite system, compared with 240 min for the selenate system. At an initial concentration of 40 ppm, again a faster ion removal was observed for selenite compared to selenate (comparing line b with d, Fig. 1). The faster removal of Se(IV) as compared to that of Se(VI) may be explained by its greater adsorption on TiO_2 and hence faster exhaustion of selenium ions from the solution. The difference

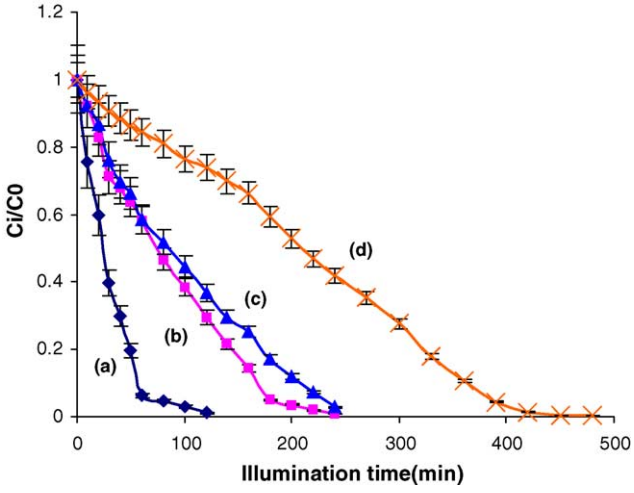

Fig. 1. Photoreduction of Se(IV) and Se(VI) in the presence of fomic acid as the hole scavenger. *Note:* C_0 being the concentration of selenium in the solution after dark adsorption; C_i: selenium concentration at time intervals. Conditions: TiO_2 loading: 1.5 g/L; pH 3.5 for Se reduction; formic acid: 300 ppm C; N_2 purging; (a) 20 ppm Se(IV); (b) 40 ppm Se(IV); (c) 20 ppm Se(VI); (d) 40 ppm Se(VI).

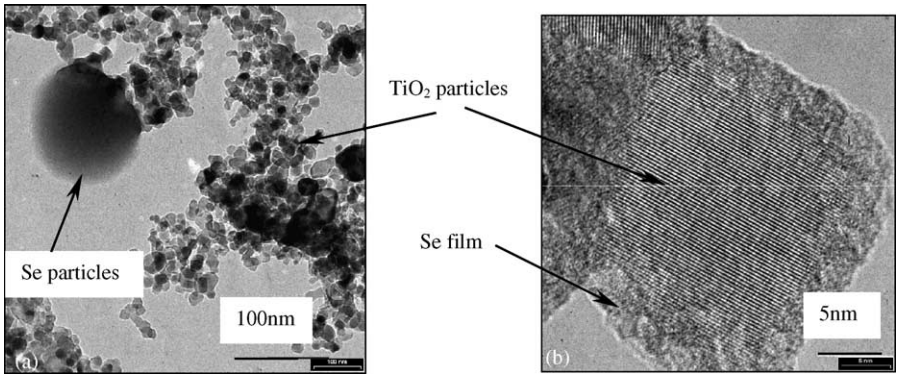

Fig. 2. TEM images of TiO_2 particles obtained after Se(IV) photoreduction. Lower magnification giving an overview of the mixed nature of the Se-modified TiO_2 powder containing both separate Se particles and Se–TiO_2 particles. Higher magnification revealing a layer of Se covering the TiO_2 particles. *Conditions*: TiO_2: 1.5 g/L; pH 3.5; dark adsorption: 20 min; initial Se(IV) concentration: 80 ppm; initial formic acid concentration: 300 ppm C.

in adsorption can be attributed to differences in the structure of the two chemical species, which affect the nature of the bonds formed during the sorption process [22–23]. The differences in the overall photoreduction rates may also lie in the fact that only four electrons are needed for the reduction of Se(IV), while six electrons are required for Se(VI) ions to be reduced.

3.2. Characterisation of Se–TiO_2 particles

3.2.1. TEM characterisation

After the photoreduction experiment of 80 ppm Se(IV), the Se–TiO_2 particles were transferred directly from the reaction suspension and placed on a carbon-coated copper grid. TEM images of the Se–TiO_2 particles at low and high magnifications are shown in Fig. 2a and b, respectively. The use of this high initial concentration of selenium ions was to have a better observation of the Se deposits.

From Fig. 2, two products of the photoreduction of selenite can be observed. The image at lower magnification (Fig. 2a) shows that the powder contained discrete spherical Se(0) particles. A closer look at higher TEM magnification (Fig. 2b) revealed an amorphous Se layer, approximately 3–4 nm thick, which had deposited on the surface of the TiO_2 particles. The two types of deposited selenium are believed to have formed by different mechanisms as will be discussed later. It should be noted that a similar observation was also obtained for the Se–TiO_2 powder recovered from the photoreduction of 80 ppm Se(VI), in which both discrete Se particles and a Se film on the TiO_2 particles were present.

3.2.2. Characterisation of optical properties

Fig. 3 shows the absorbance spectra of pure TiO_2 (line a), elemental Se powder (line b) and a physically mixture of Se and TiO_2 powders (10 wt.% Se) (line c). The elemental Se powder was prepared in-house by purging H_2Se gas, which was generated from further photoreduction of Se(0) deposited on TiO_2, into a $NaSeO_3$ solution. The particles were collected and dried in an oven at 60 °C. Fig. 4 presents the absorbance spectra of the TiO_2 powders obtained from photoreduction experiments of Se(IV) and Se(VI). These powders were also dried in the oven at 60 °C.

As can be seen from Fig. 3, the absorbance spectrum of the Se-mixed TiO_2 powder (line c) has two absorbance onsets. The onset at around 720 nm is assigned to Se. The onset at 390 nm is assigned to TiO_2, although is slightly red-shifted compared to the onset of pure TiO_2 at 380 nm. From Fig. 4, when Se(0) was deposited on TiO_2 particles using Se(IV) and Se(VI) as precursors to form a dual Se–TiO_2 semiconductor, a red shift relative to pure TiO_2 at 400 nm was observed (lines c–f). These powders also showed an absorbance onset at approximately 680 nm, which was blue-shifted relative to pure Se.

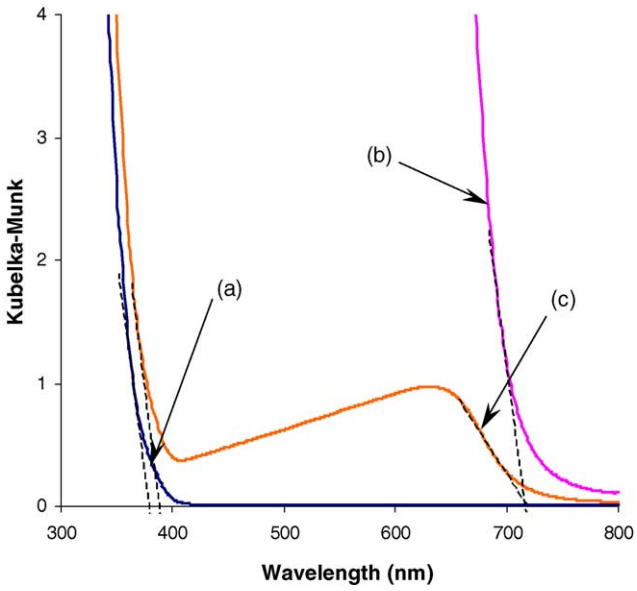

Fig. 3. Absorbance spectra of: (a) pure TiO_2; (b) pure Se; (c) physically mixed powders of 10 wt.% Se and the remainder TiO_2.

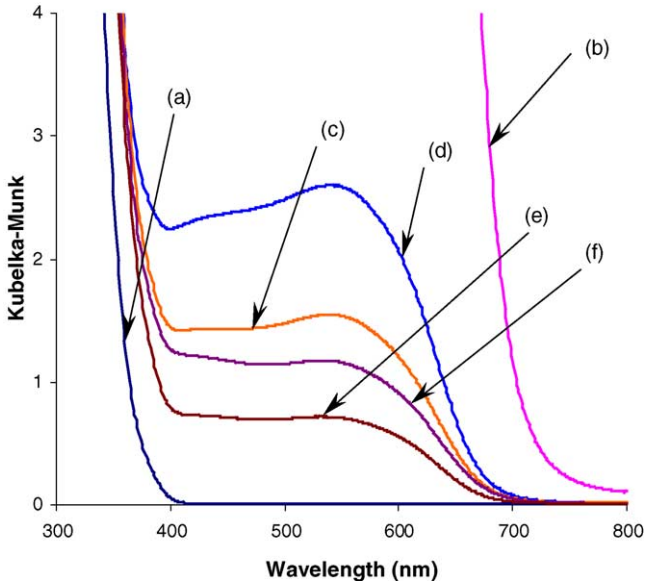

Fig. 4. Absorbance spectra of pure TiO_2, pure Se and TiO_2 recovered from photoreduction of Se(IV) and Se(VI), (a) Pure TiO_2; (b) pure Se, (c) and (d) TiO_2 recovered from the photoreduction of Se(IV) with concentrations of 20 and 40 ppm, respectively; (e) and (f) TiO_2 recovered from the photoreduction of Se(VI) with concentrations of 20 and 40 ppm, respectively. The photoreduction experiments were conducted in the presence of 300 ppm C formic acid.

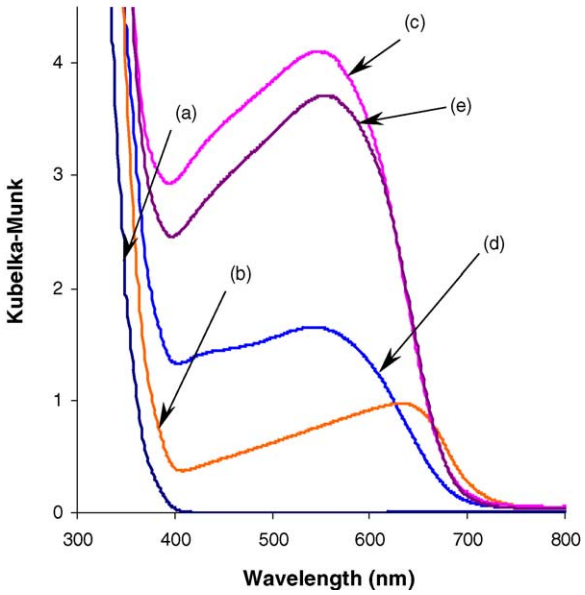

Fig. 5. Absorbance spectra of: (a) pure TiO_2; (b) physical mixture of 10 wt.% Se and TiO_2; (c) TiO_2 recovered from photoreduction of 80 ppm Se(IV) for 13 h; (d) sample c illuminated for a further 3 h; and (e) TiO_2 recovered from 80 ppm Se(VI) photoreduction for 18 h. All photoreduction experiments were conducted in the presence of 300 ppm C formic acid.

Theoretical and experimental work on II–VI core-shell particle system indicate that the bandgap energy of the system is influenced by the relative composition of the core-shell particle [24–26]. It is postulated here that the red shifts observed for Se–TiO_2 particles compared to pure TiO_2 in Fig. 4 are due to the heterojunction between the core TiO_2 particles and the Se layer and/or particles. Furthermore, the shift toward a longer wavelength that was observed for the Se-mixed TiO_2 powder in Fig. 3 may be indicative of electronic interactions even in physically mixed systems.

Injecting electrons or holes into metal particles can cause blue or red shift of the absorbance bands of the metal [27]. For example, a blue shift in the absorbance bands of silver has been reported for Ag–TiO_2 systems [28]. Se (a p-type semiconductor) and TiO_2 (an n-type semiconductor) have different Fermi level positions. When in contact, electrons from TiO_2 migrate to Se until their Fermi levels are aligned. This may explain the blue shift of the absorbance of Se.

From Fig. 4, it can also be seen that the intensity of the absorbance band of the Se–TiO_2 powders obtained increased with an increase of the Se loading (comparing line c with d and line e with f, in Fig. 4). Furthermore, the absorbance intensity of Se–TiO_2 powders obtained from Se(IV) photoreduction experiments was higher than that of the Se–TiO_2 collected from photoreduction of Se(VI) (comparing lines c–f). This was also accompanied by a decrease in the colour intensity from dark (Se(IV)) to light (Se(VI)) purple of the dried Se–TiO_2 powders, respectively. We have previously reported that the photocatalytic reduction of Se(IV) resulted in the formation of Se(0) deposits [18], which were smaller and more evenly distributed than those obtained from Se(VI) photoreduction. Hence, the differences in the distribution and morphology of the deposited Se(0) when using different Se precursors may explain the observed difference in the absorbance spectra of the resulting Se–TiO_2 particles.

Compared to the Se–TiO_2 systems shown in Fig. 4, when the initial concentration of Se(IV) and Se(VI) was increased to 80 ppm, the absorbance spectra (Fig. 5, lines c and e) had deeper valleys at around 420 nm, and higher absorbance peak at 680 nm. This indicates that more Se(0) deposits were formed with an increase of the initial concentrations of selenium ions.

Further studies involved collecting particles from an experiment, in which after 80 ppm Se(IV) was photoreduced (line c) a further illumination was conducted for 3 h. The absorbance spectrum of the resulting powder is shown as line d in Fig. 5. Comparing line d with line c in Fig. 5, it can be seen that the depth of the valley at around 420 nm and the height of the absorption starting at 680 nm decreased. This indicates that a fraction of the Se(0) deposits was removed by the photocatalytic reduction of Se(0) to Se(2−). On the other hand, the red shift, compared to the pure TiO_2 absorbance onset, and the blue shift, compared to the pure Se absorbance onset, could still be observed in line d, suggesting that there were still electronic interactions between the TiO_2 particles and Se deposits.

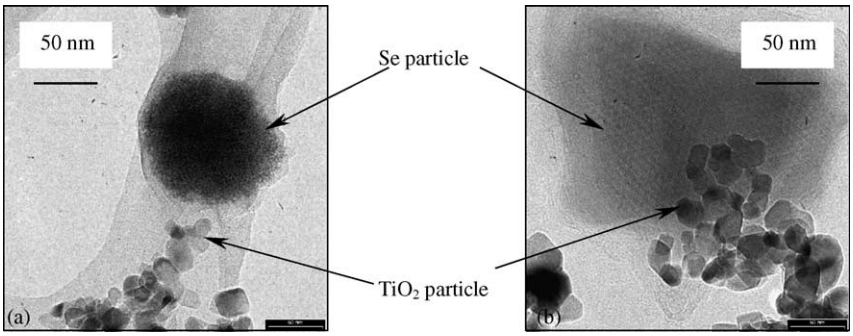

Fig. 6. TEM images of TiO_2 particles obtained after Se(IV) photoreduction, (a) wet sample; (b) sample (a) after dried in an oven at 60 °C, showing a defined structure of Se(0) particle. *Conditions*: TiO_2: 1.5 g/L; pH 3.5; initial Se(IV) concentration: 80 ppm; initial formic acid concentration: 300 ppm C; dark adsorption: 20 min; photoreduction: 8 h.

As a final note, the colour of the Se deposits will be discussed. The Se deposits formed by the photocatalytic reduction of Se ions were red in colour. For the UV–vis reflectance measurements, the particles were dried at 60 °C to form a powder that can be characterised. During this drying step, the colour of the Se–TiO_2 particles changed from orange–pink to purple. It is known that elemental selenium has different allotropic forms, of which the grey "metallic" Se, existing as hexagonal crystalline featuring helical polymeric chain, is the most thermodynamically stable [29]. It is believed that the Se(0) deposits obtained from the photoreduction reaction underwent a transformation into a crystalline form during the drying process. This was confirmed by TEM analysis as shown in Fig. 6.

3.3. An insight on the formation mechanisms of Se(0) from selenite and selenate photoreduction

It is well established that upon illumination of a TiO_2 suspension, the photogenerated holes can be scavenged by the oxidation reaction of an organic compound (in this study formic acid). In the reduction pathway, the photogenerated electrons can participate in the reduction of metal ions such as Se(IV) and Se(VI). From the results discussed so far, the following explanation for selenite and selenate photoreduction is put forward. The photoreduction of selenite is discussed first.

As can be seen from Fig. 7, in acidic conditions, the potential of the TiO_2 conduction band electrons is −0.3 V. Hence, it has enough reducing power to reduce selenite to selenium according to reaction 2 (Table 1).

In addition, the six electron reduction of Se(IV) to Se(2−) by the TiO_2 photogenerated electrons cannot be ruled out, as it is also thermodynamically feasible according to reaction (6).

$$HSeO_3^- + 6e^- + 7H^+ \rightarrow H_2Se + 3H_2O, \quad E^0 = +0.386\,V \tag{6}$$

Furthermore, when comparing the redox potential of Se(0)/Se(2−) couple with the conduction band electrons of the Se semiconductor as shown in Fig. 7, it can be seen that once Se(0) is produced, the photoreduction of Se(0) to Se(2−) can also occur. In fact, in an earlier publication [18], we attributed the further reduction of Se(0) to Se(2−) to the photogenerated electrons from the Se p-type semiconductor. This is shown as reaction 4 in Table 1.

The generation of H_2Se was only observed when the selenite was almost exhausted from the solution. The production of Se(2−) toward the end of the photoreduction of Se(IV) and Se(VI) upon illumination of TiO_2 suspensions has been previously observed [15–18]. This was explained due to insufficient reducing power of the TiO_2 photogenerated electrons to reduce Se(0) to Se(2−) [17] or the favourable photoreduction of Se(VI) to Se(0) over the reduction of Se(0) to Se(2−) by the Se photogenerated electrons [18]. However, as pointed out earlier, the photoreduction of selenite and elemental selenium to selenide is also possible. Thus, further clarification is

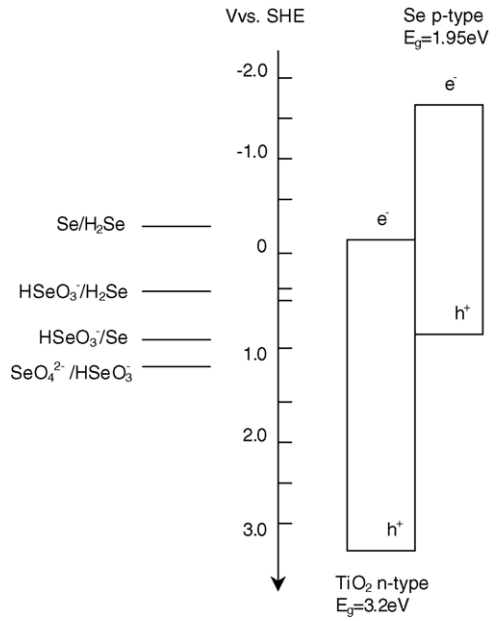

Fig. 7. Relative position of conduction and valence bands of TiO_2 and Se semiconductors, compared with redox potentials of selenium couples in acidic conditions.

needed. In the following we attempt to address this remaining question.

Hydrogen selenide has been reported to react rapidly with Se(IV) to give Se(0) via the following reaction [30–31]:

$$H_2SeO_3 + 2H_2Se \rightarrow 3Se^0 + 3H_2O \quad (7)$$

Hence, the net result of the photocatalytic reduction of Se(IV) is the production of Se(0) until the exhaustion of Se(IV). It is only then the evolution of H_2Se, due to the further reduction of Se(0) by the Se photogenerated electrons is observed.

In order to confirm the possibility of reaction (7), the following set of experiments was carried out. The setup for these experiments was similar to the setup for selenite photocatalytic reduction experiments, except that the copper ion solution in the scrubber was replaced by a sodium selenite solution. The Se(IV) photoreduction reaction was carried out as per normal procedure, and once H_2Se was generated, the gas was purged to the scrubber. Upon reaching the scrubber, now containing the sodium selenite solution, red particles were observed to gradually form, indicating the formation of Se(0). Fig. 8 shows the Se(0) particles observed under the TEM. This therefore confirmed our postulation that Se(0) particles can be formed due to the reaction between selenite and selenide ions as shown in Eq. (7).

To summarise, Se deposits of two different morphologies were formed by the photocatalytic reduction of Se(IV). It is postulated that the formation of the Se deposits was due to two reaction pathways: the first through direct reduction of Se(IV) to Se(0) by TiO_2 photogenerated electrons, and the second by the reaction between Se(2−) with Se(IV). For the second reaction, the Se(2−) ions in the solution were the result of the reduction of Se(IV) and Se(0) by the photogenerated TiO_2 electrons and/or the Se photogenerated electrons. The Se(2−) produced may diffuse away from the TiO_2 surface and react in the diffusion layer with the incoming selenite ions to precipitate elemental selenium. Using voltammetric methods to study the reduction of Se(IV), Jarzabek and Kublic [32] and Espisona et al. [33] have reported the formation of Se(0) by direct electrochemical reduction (reactions (2) and (3)) or by a chemical reaction (reaction 7). The stripping of deposited Se(0) due to further reduction of Se(0) and then redeposition of Se(0) has also been observed by Wei et al. [34]. Our study has now shown that the reaction between Se(IV) and Se(2−) did occur and produced red Se(0) particles. Therefore, we believe that in our system, the formation of discrete Se(0) particles was due to the chemical reaction between Se(IV) and Se(2−) while the direct photoreduction of Se(IV) resulted in the formation of Se(0) film/coating on the surface of TiO_2 particles (as shown in Fig. 2).

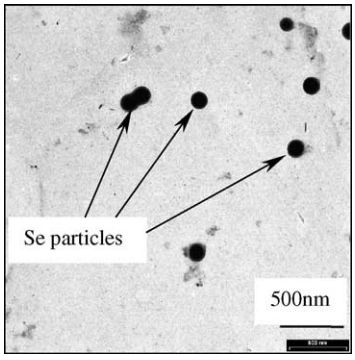

Fig. 8. Se(0) particles, recovered from scrubber containing selenite solution after H_2Se was generated, observed under TEM.

In the following discussion, we compare the photoreduction reaction of Se(IV) and Se(VI). It is clear that the latter proceeded more slowly (Table 2, Sets 4–6; Fig. 1, lines c and d). This has been attributed to the difference in the adsorption ability of the two selenium species, which resulted in faster removal of Se(IV) from solutions, compared to that of Se(VI) [18]. As the redox potential of couple Se(VI)/Se(IV) is 1.060 V (Fig. 3), Se(VI) can be first photoreduced to Se(IV) by the TiO_2 photogenerated electrons (reaction 1, Table 1). The SeO_4^{2-} species is a strong oxidising agent. However, it is known that the reduction reaction of Se(VI) to Se(IV) is usually not kinetically fast [22]. This could also limit the overall photoreduction rate of Se(VI) to Se(0). As selenite was not detected during the photoreduction of selenate [15] it can be suggested that the photoreduction of Se(IV) to Se(0) proceeded faster than the reduction of Se(VI) to Se(IV).

It should be noted that in the present discussion, the standard redox potentials in acidic condition are used as indicators of the selenium ion energy levels. Changes in the redox potentials of selenium ions may occur once they were adsorbed on TiO_2 [35]. However, this effect is unlikely to alter our overall picture of the mechanism for the photoreduction of selenium ions.

4. Conclusions

Upon UV illumination, selenite and selenate were photoreduced to their elemental form (Se(0)) when using TiO_2 as the photocatalyst and formic acid as the hole scavenger. Both discrete Se particles and films were observed to have formed on the surface of the TiO_2 particles. In addition, UV–vis reflectance measurements showed that the Se–TiO_2 particles demonstrated a red shift, as compared to pure TiO_2. An additional absorbance onset at 680 nm was also observed and attributed to the presence of the purple crystalline Se(0) deposits. The deposition of Se(0) coating was explained in terms of the direct reduction of Se(IV) and Se(VI) by the TiO_2 photogenerated electrons upon illumination. Furthermore, a reaction between Se(2−) and Se(IV) is believed to have contributed to the formation of discrete Se(0) particles.

Acknowledgements

We would like to thank the academic and technical staff from the School of Chemical Science, UNSW for their assis-

tance with using the UV–vis Cary 5 instrument, and the Electron Microscope Unit, UNSW for their assistance with the use of TEM. Vi N.H. Nguyen would also like to acknowledge AusAID for the scholarship provided for her Ph.D. study.

References

[1] U. Tinggi, Toxicol. Lett. 137 (2003) 103–110.
[2] F. Seby, M. Potin-Gautier, E. Giffaut, G. Borge, O.F.X. Donard, Chem. Geol. 171 (2001) 173–194.
[3] A.D. Lemly, Ecotoxicol. Environ. Safe 59 (1) (2004) 44–56.
[4] A. Kapoor, T. Tanjore, T. Viraraghavan, Environ. Sci. Technol. 49 (1995) 137–147.
[5] J.V. Boegal, D.A. Clifford, EPA/600/2-86/031, EPA Publication, Cincinnati, OH, 1986.
[6] Chemical separation with liquid membranes, in: K.J. Gleason (Ed.), Removal of Selenium from Contaminated Waters using Emulsion Liquid Membranes, American Chemical Society, Washington, DC, 1996, pp. 342–360 (Chapter 24).
[7] Y.K. Kharaka, Appl. Geochem. 11 (1996) 797–802.
[8] A. Murphy, Ind. Eng. Chem. Res. 27 (1988) 187–191.
[9] S.C.B. Myneni, T.K. Tokunaga, G.E. Brown Jr., Science 278 (1997) 1106–1109.
[10] P. Refait, L. Simon, J.R. Genin, Environ. Sci. Technol. 34 (2000) 819–825.
[11] S.R. Qiu, H.F. Lai, J. Roberson, M.L. Hunt, C. Amrhein, L.C. Giancarlo, G.W. Flynn, J.A. Yarmoff, Langmuir 16 (2000) 2230–2236.
[12] M. Fujita, M. Lke, S. Nishimoto, K. Takahashi, M. Kashiwa, J. Ferment. Bioeng. 83 (1997) 517–522.
[13] C. Garbisu, T. Ishii, T. Leighton, B.B. Buchanan, Chem. Geol. 132 (1996) 199–204.
[14] D.T. Maiers, P.L. Wichlacz, D.L. Thompson, D.F. Bruhn, Appl. Environ. Microbiol. 54 (1988) 2591–2593.
[15] S. Sanuki, T. Kojima, K. Arai, S. Nagaoka, H. Majima, Metall. Mater. Trans. B 30B (1999) 15–20.
[16] S. Sanuki, K. Shako, S. Nagaoka, H. Majima, Mater. Trans. JIM 4 (2000) 799–805.
[17] E. Kikuchi, H. Sakamoto, J. Electrochem. Soc. 147 (12) (2000) 4589–4593.
[18] T.Y.T. Tan, M. Zaw, D. Beydoun, R. Amal, J. Nanoparticle Res. 4 (6) (2002) 541–552.
[19] T.T.Y. Tan, D. Beydoun, R. Amal, J. Mol. Catal. A: Chem. 202 (2003) 73–85.
[20] T.T.Y. Tan, D. Beydoun, R. Amal, J. Phys. Chem. B 107 (2003) 4296–4303.
[21] T.T.Y. Tan, D. Beydoun, R. Amal, J. Photochem. Photobiol. A: Chem. 159 (2003) 273–280.
[22] A.F. Cotton, G. Wilkinson, The group VIA (16) elements: S, Se, Te, Po, in: Advances in Inorganic Chemistry, fifth ed., Wiley-Interscience Publication, John Wiley & Son, New York, Chichester, Brisbane, Toronto, Singapore, 1988, pp. 491–543.
[23] S. Sharmasarkar, G.F. Vance, Adv. Environ. Res. 7 (2002) 87–95.
[24] A.R. Kortan, R. Hull, R.L. Opila, M.G. Bawendi, M.L. Steigerwal, P.J. Carroll, L.E. Brus, J. Am. Chem. Soc. 112 (1990) 1327–1332.
[25] J.W. Haus, H.S. Shou, L. Honma, H. Komiyama, Phys. Rev. B 47 (1993) 1359–1365.
[26] S.H. Elder, F.M. Cot, Y. Su, S.M. Heald, A.M. Tyryshkin, M.K. Bowman, Y. Gao, A.G. Joly, M.L. Balmer, A.C. Kolwaite, K.A. Magrini, D.M. Blake, J. Am. Chem. Soc. 122 (2000) 5138–5146.
[27] A. Henglein, Ber. Bunsenges. Phys. Chem. 101 (1997) 1562–1572.
[28] Y. Zhou, C.Y. Wang, H.J. Liu, Y.R. Zhu, Z.Y. Chen, Mater. Sci. Eng. B67 (1999) 95–98.
[29] N.N. Greenwood, A. Earnshaw, Selenium, tellurium and polonium, in: Chemical Elements, second ed., Butterworth-Heinemann, 1997, pp. 747–788 (Chapter 16).
[30] A.M. Kressin, V.V. Doan, J.D. Klein, M.J. Sailor, Chem. Mater. 3 (1991) 1015–1020.
[31] M. Bouroushian, T. Kosanovic, Z. Loizos, N. Spyrellis, Electrochem. Commun. 2 (2000) 281–285.
[32] G. Jarzabek, Z. Kublic, J. Electroanal. Chem. 114 (1980) 165–177.
[33] A.M. Espisona, M.L. Tascon, M.D. Vazquez, P.S. Batanero, Electrochim. Acta 37 (1992) 1165–1172.
[34] C. Wei, N. Myung, K. Rajeshwar, J. Electroanal. Chem. 375 (1994) 109–115.
[35] A. Taghizadeh, M.F. Lawrence, L. Miller, M.A. Anderson, N. Serpone, J. Photochem. Photobiol. A: Chem. 130 (2000) 145–156.